PCCP

Accepted Manuscript

ROYAL SOCIETY OF CHEMISTRY

www.rsc.org/pccp

Journal Name

ARTICLE

Molecular Dynamics Simulation of Organohalide Perovskite Precursors: solvent effects in the formation of Perovskite solar cells

Received 00th January 20xx,
Accepted 00th January 20xx

DOI: 10.1039/x0xx00000x

www.rsc.org/

Juan José Gutierrez-Sevillano[a], Shahzada Ahmad[b], Sofía Calero[a], Juan A. Anta[a,*]

The stability and desirable crystal formation of organohalide perovskite semiconductors is of utmost relevance to ensure the success of perovskites in photovoltaic technology. Here in we have simulated the dynamics of ionic precursors toward the formation of embryonic organohalide perovskite $CH_3NH_3PbI_3$ units in the presence of solvent molecules using Molecular Dynamics. The calculations involved, a variable amount of Pb^{2+}, I^-, and $CH_3NH_3^+$ ionic precursors in water, pentane and a mixture of these two solvents. Suitable force fields for solvents and precursors have been tested and used to carry out the simulations. Radial distribution functions and mean square displacements confirm the formation of basic perovskite crystalline units in pure pentane - taken as a simple and archetypical organic solvent. In contrast, simulations in water confirm the stability of the solvated ionic precursors, which prevents their aggregation to form the perovskite compound. We have found that in the case of water/pentane binary solvent, a relatively small amount of water did not hinder the perovskite formation. Thus, our finding suggests that the cause of the poor stability of perovskite films in the presence of moisture is a chemical reaction, rather than the polar nature of the solvents. Based on the results, a set of force-field parameters to study from first principles perovskite formation and stability, also in the solid phase, is proposed.

Introduction

The discovery that organohalide perovskites are efficient light harvesters in the visible range[1] initiated its use as base material for perovskite solar cells (PSC).[2] This technology has demonstrated an impressive potential to achieve high energy conversion efficiencies, with a certified record exceeding 20% up to date.[3] These materials not only absorb light efficiently in the visible range due to its direct band gap ($CH_3NH_3PbI_3$ =1.55 eV), but also exhibit a huge dielectric constant, strong polarization and ionic migration under illumination or electrical bias.[4,5] These remarkable features facilitates the splitting of excitons at ambient temperature and the generation of free carriers. Furthermore, organohalide perovskites are capable of transporting electrons and holes without substantial recombination losses, which explains diffusion lengths in the order of 100-1000 nm for these compounds.[6,7]All these properties make organohalide perovskites ideal materials for photovoltaics. In spite of all these favourable features, PSCs have some drawbacks that hinder their commercial application. For instance, the most efficient perovskite formulation contains lead, which is a very toxic material. Widely used organohalide perovskites in PSCs are alkylammonium lead halides like $CH_3NH_3PbI_3$, constituted by organic cations at the center of the cages formed by a framework of PbI_6 octahedra. These compounds are very sensitive to the presence of moisture, degrading quickly in humid conditions. This brings serious concerns for stability due to the back formation of PbI_2 from the photoactive perovskite. Most of the practical problems that come up in the fabrication of PSCs are connected to the reversibility of the chemical process:

$$CH_3NH_3I + PbI_2 \leftrightarrow (CH_3NH_3^+ + Pb^{2+} + 3I^-) \leftrightarrow CH_3NH_3PbI_3$$

This feature makes the perovskite material to convert back to its precursors (CH_3NH_3I + PbI_2) if the ambient conditions are unfavorable. That is apparently the case in the presence of moisture and/or a liquid hole conductor, or with the rise in temperature.[8] Furthermore, the delicate formation of the perovskite also introduces reproducibility problems as a careful combination of solvents,[9] sequential applications[10] and proportions[11] of the different precursors is required to achieve a controlled and adequate morphology capable to produce champion efficiencies. For all these reasons we could refer to the PSCs as “giants with a feet of clay”, that is, a technology with a huge potential but that still lacks of a definitive chemical formulation that is both robust and efficient for solar energy conversion.

[a] Área de Química Física, Universidad Pablo de Olavide, Sevilla, Spain.
[b] Abengoa Research, Abengoa, C/Energía Solar n° 1, Campus Palmas Altas, 41014 Sevilla, Spain

† Footnotes relating to the title and/or authors should appear here.
Electronic Supplementary Information (ESI) available: Figures S1-S8 and Tables S1-S2, including force-field parameters, diffusion coefficients and extra data for RDFs and MSDs. See DOI: 10.1039/x0xx00000x

In this paper we present a Molecular Dynamics (MD) study of the embryonic formation of $CH_3NH_3PbI_3$ units from its ionic precursors ($CH_3NH_3^+$ + Pb^{2+} + I^-) in two different solvents: water and pentane. Pentane was chosen due to its ideal nature as organic, fully hydrophobic solvent to study *pure* polarity effects. Modeling of organohalide perovskite compounds was previously carried out by *ab initio* Density Functional Theory (DFT).[12] However, quantum mechanical calculations are computationally very demanding, which limits the application of these techniques to very small samples, comprising few molecules. The use of DFT or reactive force fields[13] would catch bond and polarization effects in solid formation, but at a large computational cost[14]. In contrast, MD makes it possible to simulate samples with thousands of atoms, so that concentration and solvent effects can easily be pointed out. Classical Molecular Dynamics with simple Lennard-Jones potentials and point charges have already been used to study the early stages of crystal formation from solution for a variety of materials.[15–21] However, this technique has not been used so far to study the formation of organohalide perovskites for solar cells.

The main objective of the present study is to set up a computational procedure that is capable to recreate realistically the formation of embryonic perovskite units in different chemical environments. Once this is established, it can be used to study different formulations and compositions, of both precursors and solvent, in order to predict the most adequate formulation. Additionally, this can help to identify the underlying molecular origin of the stability issues. On the other hand, MD provides a way to study correlations between the ionic building blocks of the perovskite, i.e., PbI_6 octahedra and $CH_3NH_3^+$ cations. These correlations are essential to understand the anomalous dielectric phenomena[4] and ferroelectric properties[22] of photovoltaic perovskites.

METHODOLOGY: MOLECULAR DYNAMICS OF PEROVSKITE PRECURSORS IN SOLUTION

To model the molecular species involved in the simulations we used different sets of Lennard-Jones (L-J) parameters and electrostatic potentials based on electric point charges. Water was modeled as a flexible full atom model based on the 3-point model SPC/E[23] and using the parameters coming from GROMOS 53A6[24]. The modelling for pentane was made using the flexible united-atom TraPPE model.[25] Validation of these force fields was done by NPT simulations for the pure solvents at atmospheric pressure in order to obtain the liquid density of the solvents. The equilibrium densities obtained were 1034.7 and 630.3 kg/m^3 for water and pentane respectively, which compare very well with the experimental values 997.05 and 620.83 kg/m^3 (NIST database[26]). $Pb^{2+}$and I^- were modeled as a single L-J interaction centers with partial charges and the L-J parameters were taken from Refs.[27] and [28] respectively. $CH_3NH_3^+$ was modeled using a rigid full atom model where atomic positions were taken from the open chemistry database[29], Lennard-Jones parameter from AMBER forcefield[30] and partial charges from chemistry division of Colby college[31].The validity of the molecular model used for $CH_3NH_3^+$ was verified by reproducing the results of Meng and Kollman[32] which proved to reproduce the experimental solvation enthalpies in water solutions of $CH_3NH_3^+$ salts. Our simulations with the SPC/E model accurately reproduced the nitrogen-water and carbon-water radial distribution functions (RDF) (see ESI, Figure S2). On the other hand, the model used for iodide ions was recently found to reproduce remarkably well experimental diffusion coefficients in a variety of solvents.[33] The model for lead cations was found to reproduce experimental Gibbs Free energy of Hydration[27]. All these results and cross-checks ensure that the molecular models and potential parameters used in the simulations, although simple, are adequate and that valuable information about the formation of the perovskite *in solution* can be obtained. However, the results are found not to reproduce exactly the structure of a perfectly crystalline $CH_3NH_3PbI_3$ for the aggregates produced in solution. For this reason more simulations were run in pure pentane for a new set of parameters where the correct interatomic distances in the solid phase are correctly reproduced. All L-J parameters and charges are collected in the ESI.

MD simulations comprising $CH_3NH_3^+$, Pb^{2+}, and I^- ions and solvent molecules were carried out in the NPT and in the NVT ensembles using the GROMACS simulation package.[34]
The calculations were performed in a cubic simulation box of size 3.8 × 3.8 × 3.8 nm^3 with periodic boundary conditions. This corresponds to a precursor concentration of 0.3-1.5 M. The Ewald method was used to deal with the long-range electrostatic forces. Cut-offs for the coulombic and van der Waals interactions were set to 1.2 nm. The size of the simulation box was determined by running NPT simulations at standard conditions for solvents and fixing the number of water and pentane molecules to 1820 and 287 respectively. That was found to reproduce the experimental densities of these two solvents at standard conditions. The pure solvent system was then added with 10, 20, 30, 40 and 50 ($CH_3NH_3^+$, Pb^{2+}, 3×I^-) precursor units in their stoichiometric proportion in the $CH_3NH_3PbI_3$ compound. Simulations with $CH_3NH_3PbI_3$ precursors were carried out in the NVT ensemble with the afore-mentioned number of solvent molecules. An additional simulation with a 10/90 water/pentane mole ratio was performed. This involved 35 and 282 water and pentane molecules in a single simulation box including 20 ($CH_3NH_3^+$, Pb^{2+}, 3I^-)-units. The time step used was 0.5 fs, and the total simulated time including equilibration was 10.250 ns.

Results and Discussions

Radial distribution functions from solvent-oriented force-field

The equilibrated MD simulations for 20 $CH_3NH_3PbI_3$ precursors in pure water and in pure pentane are shown in **Figure 1**. The most notable observation is that precursor ions tend to aggregate in pentane whereas in water they remained fully dispersed and solvated. This is not surprising given the ionic nature of the precursors and the polar character of the water molecules. It was also observed that the clustering remains in time and that the aggregates were not destroyed by the solvent molecules.

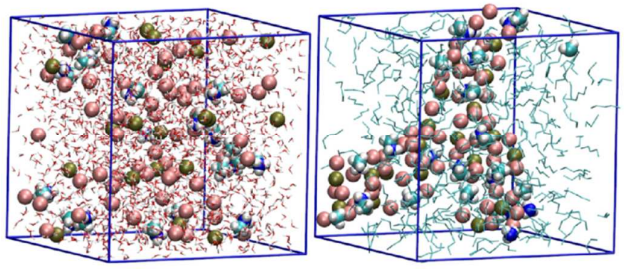

Figure 1 Snapshots of equilibrated MD simulations with 20 $CH_3NH_3PbI_3$ precursors in water (left) and in pentane (right). Balls are used to represent the precursor species (I pink, Pb tan, C cyan, N blue, and H white) and a stick-model is used to represent solvent molecules.

The aggregation in the presence of the organic solvent (and its absence in water) is confirmed when the RDFs are extracted from the simulations. The RDF is defined as the thermodynamic average of the two-particle correlation function relative to that of a non-interacting system[35]

$$g(r) = \frac{1}{\rho}\langle \sum_{i\neq 0} \delta(\vec{r} - \vec{r}_i)\rangle = V\frac{N-1}{N}\langle \delta(\vec{r} - \vec{r}_i)\rangle \quad (1)$$

where ρ, V and N are the density, the volume and the number of particles of the system, respectively, and **r** refers to the atomic positions. In **Figure 2** the Pb-CH_3NH_3 and Pb-I RDFs are reported. It is clearly observed that in water there is practically no correlation between lead and the organic cations (RDF close to 1). On the contrary, for pentane, a clear first coordination peak is detected, in spite of the like positive charge of both species. Accordingly, the coordination is more pronounced for the Pb-I interaction. In the presence of pentane, the first coordination peak reaches a value of around 100, which leads to a coordination number (obtained by spherical cumulative integration of the RDF with respect to distance) of around 5 iodide ions. Although PbI_6 octahedra, characteristic of organohalide perovskites, are not formed in the hydrophobic medium created by the pentane molecules for this force-field, the occurrence of stable PbI_x units is clearly observed in the simulations performed in the hydrophobic medium created by the molecules of pentane. This observation is in line with the formation of PbIx complexes in precursor solution, which has been recently reported by several groups.[11,36] It is interesting to compare the position of the peaks with the interatomic distances obtained from crystallographic data[37] of solid $CH_3NH_3PbI_3$. These distances are represented by vertical lines in the figures. Whereas for water the first peak falls far from the crystallographic distance, in pentane the Pb-I first peak lies quite close to the crystal position, showing that genuine perovskite formation is induced by the presence of pentane molecules. Similar results were also obtained for the rest of the correlations as shown in the ESI (Figure S3 of the ESI). Although the solvent-oriented force-field does not gives perfect matching of the crystallographic distances and no PbI_6 octahedra are found, we show next that a refinement of the parameters leads to matching of the crystalline structure. Results for this solid-oriented force-field are presented in the last section.

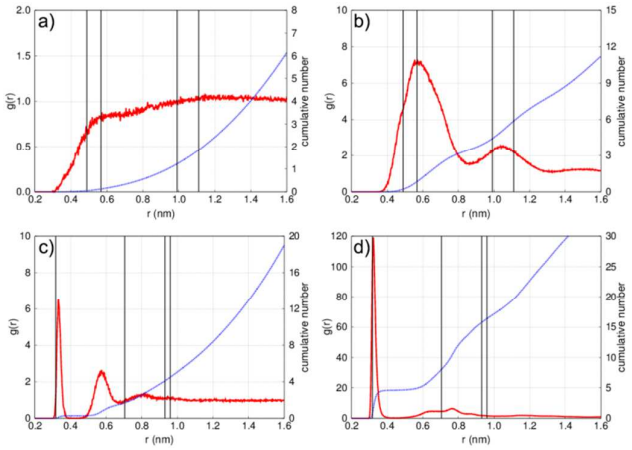

Figure 2. RDFs (red line) and coordination number (blue dotted line) for Pb^{2+}-$MeNH_3^+$ (top) and Pb^{2+}-I^- (bottom) from equilibrated MD simulations with 20 $CH_3NH_3PbI_3$ precursors in water (left) and in pentane (right). Blue lines correspond to the cumulative sum of the RDF (coordination number). Vertical lines stand for the crystallographic positions of solid $CH_3NH_3PbI_3$ obtained from Ref.[37]

As the RDF is an indicative of the strength of the statistical correlation between molecular species in an equilibrated system, it is worthy to study the magnitude of the peaks shown by these functions. **Figure 3** shows the RDFs between species in pentane Pb^{2+}-Pb^{2+} ad I^--I^- RDFs exhibit strong short-range correlations in the form of high first-coordination peaks near its crystallographic positions. In the case of the iodide-iodide interaction, only the first-coordination peak falls close to the crystal position inside the PbI_6 octahedra whereas two peaks appear for the lead-lead interaction, one of them close to the crystal position. The occurrence of the high Pb^{2+}-Pb^{2+} first-coordination peak suggests that the correlation between PbI_x units, although not as strong as within the octahedra (Figure 2d), is quite robust. As a matter of fact, the integration of the RDF gives a clear plateau at around 3 units, indicating that each PbI_x unit surrounds itself by 3 neighbors, two of them at the crystallographic distance.

In striking contrast to the rest of the RDFs, the correlation between the $CH_3NH_3^+$ ions is relatively weak, as can be inferred from the height and width of the peak. This suggests that the organic cations are less correlated than the rest of the components of the perovskite. Lead and iodide ions tend to

"freeze" in a relatively robust PbI_x-PbI_x framework and, the microscopic structure of the methylammonium cations remains more liquid-like. In a recent publication[11], Yan and coworkers discussed the formation of the perovskite in terms of an intermediate "soft-colloidal" state in which a PbI_x-PbI_x framework is first formed, within which the methylammonium ions are subsequently incorporated. The predictions of the MD simulations in hydrophobic medium are therefore consistent with these experimental observations.

There is also a quite important aspect that can be inferred from the observed different correlation strength of Pb-Pb and $CH_3NH_3^+$ - $CH_3NH_3^+$ interactions. This explains the strong molecular dielectric response of the perovskite material and the possibility of ion migration[5]under illumination and in the presence of external fields.[4,38] These two properties have been claimed as the cause of hysteresis[39,40] in the measurement of the current-voltage curve. As methylammonium cations have a strong polar character due to the localization of the positive charge near the nitrogen atom, they tend to re-orient and re-organize within the PbI_x-PbI_x framework under the application of an external electric field. A similar effect takes place upon illumination, as the photogeneration of free carriers creates local electric fields that modify the microscopic structure of the material.[40] This has been pointed out as the reason of the low recombination rates found in these materials31, as electrons and holes tend to remain further apart in the polarized structure due to the occurrence of local electric fields, hence preventing their self-annihilation.

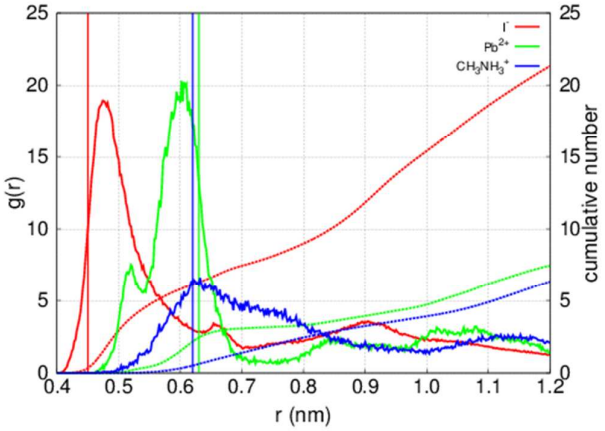

Figure 3. RDFs (solid lines) and coordination number (dotted lines) between like species ([CH3NH3]+ blue, Pb2+ green, and I- red) obtained from equilibrated MD simulations with 20 CH3NH3PbI3 precursors in pentane. Vertical lines stand for the crystallographic positions of solid CH3NH3PbI3 as reported in Ref.37

MD simulations for different precursor concentrations were carried out to mimic the effect of solvent evaporation that is commonly used[10] to deposit active perovskite films onto substrates. Results can be found in the ESI (Figures S4 and S5). In spite of the different concentrations used, the RDFs show a very similar structure for water solutions, except for the largest concentration, where Pb-I pairs are detected. Contrary to the case of water, in pentane, where perovskite formation has already been discussed, the magnitude of the first-coordination peak is very concentration-dependent. However, the formation of the PbI_x units is clearly seen in all cases, as evidenced by the cumulative integration of the RDF, which gives coordination numbers close to 5 up to intermediate distances. Although the short-range correlation was found to be stronger for lower concentrations, the cumulative sum at long distances is only an increasing function if the number of precursors exceeds a certain concentration threshold. This result suggests that at low concentrations the precursors tend to form isolated units involving just the first coordination shell. In contrast, an increase of the concentration favors the formation of larger aggregates and the initial stage of a colloidal phase leading to a macroscopic perovskite crystalline structure, as mentioned above.[11] This behavior hence reflects the effect of solvent evaporation that leads to the triggering of perovskite formation.

Dynamical properties from solvent-oriented force-field

MD simulations have the advantage of providing results for dynamical properties as well. In this line, we have extracted the mean square displacement (MSD) of precursor species and solvent molecules as a function of time. This is defined as a statistical average of the relative positions of particles in the simulation

$$\langle r(t)^2\rangle = \frac{1}{N}\sum_{1=1}^{N}\{[x_i(t)-x_i(0)]^2+[y_i(t)-y_i(0)]^2+[z_i(t)-z_i(0)]^2\} \quad (2)$$

where *i* is an index that runs over the total number of particles of each type *N*. The MSD has the following time dependence[42]

$$r(t)^2 = 2dD_s t^{\propto} \quad (3)$$

where *d* is the dimensionality of the system and D_s is the self-diffusion coefficient. α is a power exponent that reflects the nature of the atomic motion: for normal diffusion $\alpha = 1$ whereas $\alpha \neq 1$ is an indicative of *anomalous* diffusion. Values of $\alpha < 1$ (subdiffusion) usually signal processes of aggregation, "freezing" or glass transitions. A double logarithmic plot of the MSD permits to extract α from the slope of the curve. Results for the MSD are reported in **Figure 4** in both linear and double logarithmic plots.

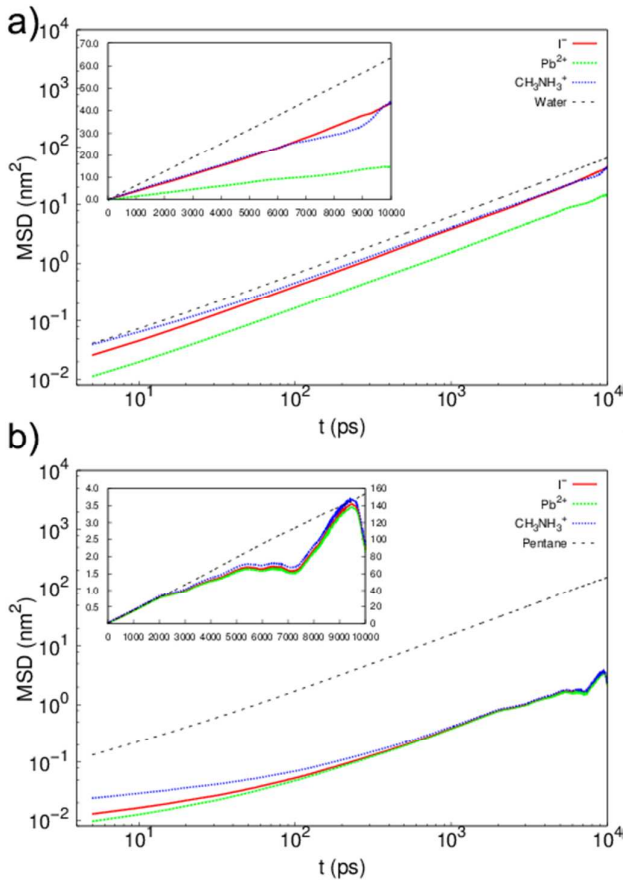

Figure 4 Mean Square Displacements (MSD) for precursor species and solvent molecules as obtained from MD simulations with 20 precursors in water (top) and in pentane (bottom)

The MSDs show normal diffusion behavior in water for all precursors with α ranging between 0.93 and 1.00 (Table S2 in the ESI). From the intercepts of the lines in the log-log plot (or the slope in the linear plot) the diffusion coefficient can be estimated. Water, iodide and methylammonium show similar diffusivity (~ 0.5-1 10^{-3} m^2/s), while lead ions tend to diffuse more slowly. This is likely related to the solvation of lead ions by water molecules, which is much stronger for Pb^{2+} than for the rest of the species (Figure S6 in the ESI). In pentane the diffusion behavior is radically different. Whereas the solvent molecules diffuse rapidly and with normal diffusion behavior (α ~ 0.89-0.97), the motion of the ionic precursors tend to slow down as the simulation proceeds (α ~ 0.5-0.95). Interestingly, the MSDs of the three precursor species tend to converge at long times. For times beyond 1-10 ns, the displacement of all ions is nearly coincident. We consider this effect as a strong indication of clustering in the hydrophobic medium, in agreement with the static data shown above. We have also studied the diffusion for varying concentrations of precursors (Figure S7 in the ESI). In analogy to the results for the RDFs, the diffusion dynamics is roughly independent of the concentration for water. In contrast, the MSDs obtained for pentane are smaller for increasing concentrations, which confirms that the aggregation to form the perovskite is favored when the precursor/solvent ratio is increased (like in an evaporation experiment).

We calculated velocity autocorrelation functions (VAF), defined by the statistical average of scalar products of particle velocities[35]

$$C(t) = \langle \vec{v}(0) \cdot \vec{v}(t) \rangle \qquad (4)$$

Results for VAFs are presented in **Figure 5**. The main difference between water and pentane is the shape of the function. For the organic solvent, the precursor VAFs have the typical solid-like shape (damped harmonic), whereas pentane behaves as a simple weak-interacting liquid (pure exponential decay) due to loss of correlations at longer times. In water all VAFs indicate liquid structure, water included. This shows that there is only short-range order, typical of an associated liquid. The oscillating behavior showed by the precursors in pentane confirms the formation of solid-like perovskite units as demonstrated before.

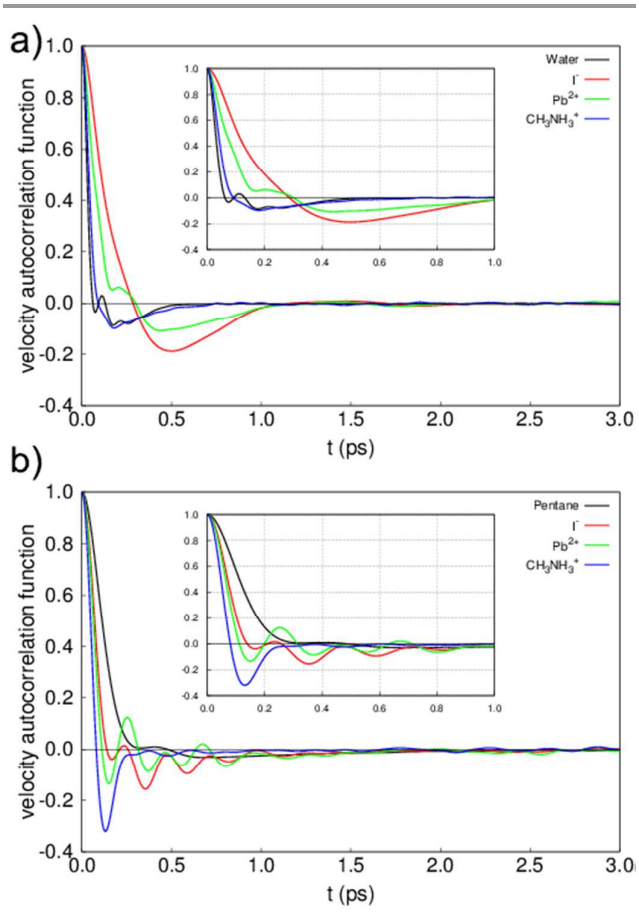

Figure 5. Velocity Autocorrelation Functions (VAFs) for precursor species ([CH_3NH_3]$^+$ green, Pb^{2+} pink, and I^- blue) and solvent molecules (red line) as obtained from MD simulations with 20 precursors in water (top) and in pentane (bottom)

Sensitivity of water content to perovskite formation

One of the main drawbacks of PSCs is their tendency to degrade in humid conditions. To address this issue, we have carried out MD simulations for a water/pentane blend, where water is the minority component. Results for a 10% mole concentration of water are presented in **Figure 6**.

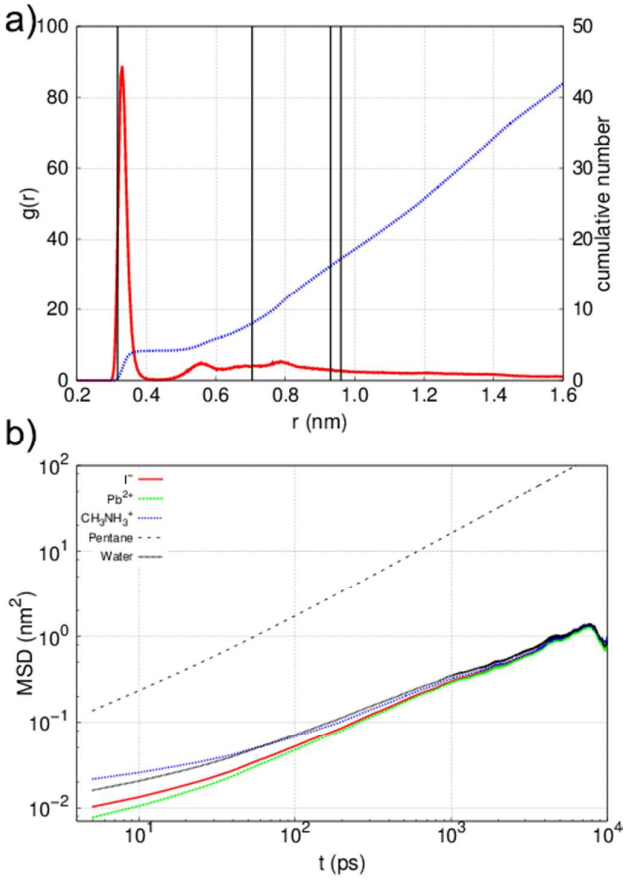

Figure 6. **Top:** Pb-I RDF (red line) and coordination number (blue dotted line). Vertical lines stand for the crystallographic positions of solid $CH_3NH_3PbI_3$ obtained from Ref.[26] **Bottom:** MSDs for all species ($[CH_3NH_3]^+$ red, Pb^{2+} blue, I^- green, pentane black line, and water dashed line) as obtained from a MD simulation with 20 precursors and 10/90 mol ratio water/pentane.

The MD simulations for the 10/90 blend indicate that the small amount of water used does not prevent the aggregation of the precursors and the formation of the basic PbI_x units. The first peak of the Pb-I RDF reaches a height of ~90, close to 120, which is the value obtained for pure pentane (Figure 2). Furthermore, the behavior of the MSDs, is very similar to that found in pure pentane (Figure 4), that shows the clustering of the precursors at around 10 ns. Thus, the polar nature of water is not sufficient to prevent the formation of the perovskite structure when it is added in small quantities. As it is well-known that perovskite films are extremely sensitive to the presence of moisture, we can infer in all like hood that it is a chemical reaction and not the polarity of the environment the reason of the poor stability of perovskite film in ambient conditions. In fact, the formation of hydrates has been recently reported in the literature as a source of chemical instability.[43,44] The formation of hydrates or any other chemical reaction that involves the formation of covalent bonds is not easily attainable by simple MD methods and require more sophisticated force-fields.[13] Another possibility is that water is more critical when accompanied by other solvent such as DMF or γ-Butyrolactone. Simulations and modeling to study and analyse these systems are currently underway.

Solid-oriented force-field

As discussed before, the force-field that describes correctly the behaviour of the precursors in solution does not give a perfect crystal for the cases where there is aggregation, i.e., in pentane. For instance, PbI_6 octahedra are not naturally occurring in the simulation (a coordination number close to 5, rather than to 6 is found for the Pb-I RDF of Figure 2d). Furthermore, the interatomic distances do not coincide exactly with the reported values for crystalline $CH_3NH_3PbI_3$. For this reason we have attempted a refinement of the solvent-oriented force-field used in the aggregation studies so that a more accurate description of the perovskite in its solid phase is accomplished.

For refinement of the force field parameters the most obvious candidates are the σ-values. In contrast, ε-values, dealing with Van der Waals interactions, are hidden behind the much stronger coulombic attraction. On the other hand, charges were kept fixed for simplicity (-1 and +2 for iodide and lead ions, respectively). Hence, we have systematically vary the σ-parameter of I^- and Pb^{2+} and measure the Pb-I coordination number obtained for the aggregate state in pentane. Results can be found in **Figure 7** and in the ESI (Figure S8).

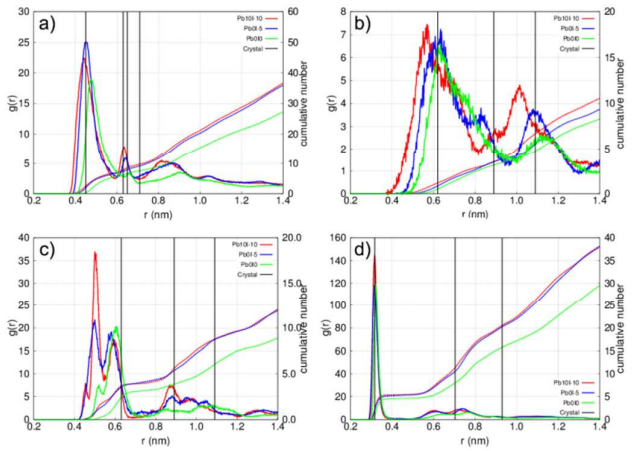

Figure 7. RDFs (solid lines) and coordination number (dotted lines) from MD simulations with 20 precursors in pentane and different choice of σ-parameters for Pb2+ and I-. Vertical lines stand for the crystallographic positions of solid CH3NH3PbI3 obtained from Ref.37 Correlations shown correspond to I-I (top left), CH3NH3-CH3NH3 (center-of-mass, top right), Pb-Pb (bottom left) and Pb-I (bottom right). Labels are in the format PbxI-y, where x stands for the percentage increase of the σ-

parameter of Pb2+ and y for the percentage decrease of the σ-parameter of I- with respect to the solvent-oriented forced field utilized in the simulations shown in Figures 2 and 3.

Figure S8 shows that either decreasing the size of the iodide anions or increasing the size of the lead cations leads to an increase of the Pb-I coordination number. In particular, two combinations of parameters are found to produce a coordination number above 5.4 (close to the ideal PbI_6 octahedral structure characteristic of solid perovskite). These combinations are: (A) concurrent modification of the Pb and I σ-parameters (10% positive and negative, respectively) and (B) a 5% reduction of the σ for I, keeping Pb unaltered). However, both choices are not equivalent when we look at the rest of the correlations, as inferred from **Figure 7**. The 5% reduction of the σ-parameter for I gets a better estimation of the crystallographic distances for both the I-I and CH_3NH_3-CH_3NH_3 distances. On the other hand, both combinations also improve the Pb-Pb and Pb-I distance estimation and make the Pb-Pb coordination number closer to the ideal value of 6. Based on these observations, we conclude that just a small variation of the iodide σ parameter with respect to the solution-oriented force-field is the most convenient choice to get an adequate short-range description of the crystalline structure of solid $CH_3NH_3PbI_3$. To add further support to the suitability of the proposed force field, we have performed an additional simulation of 20 precursor units initially placed in their crystallographic positions, and in the presence of pentane. The results (see Figures S9 and S10 in the ESI) show that the solid remains stable, and the correct interatomic distance remain oscillating around the crystallographic positions. All these results demonstrate the capability of the Lennard-Jones potential to catch, in an average manner,[45] the complex bond and polarization effects taking place in real systems.

Conclusions

We have studied the process of perovskite formation from its ionic precursors using MD simulations with suitable force fields. The results show clear clustering of precursors and formation of basic perovskite units (like PbI_x units) for the simulations run in model organic solvent, i.e., pure pentane. The formation of the basic perovskite structure is confirmed by the radial distribution functions extracted from the equilibrated simulations, whereas mean square displacements indicated that aggregation takes place in pure hydrophobic medium in a time interval of 1-10 ns. The microscopic structure derived from the simulations shows that the correlation between methylammonium units is much weaker than between lead and iodide ions, a feature that connects with the ferroelectric properties and slow dynamic dielectric and ion migration processes reported for this kind of compounds.

Simulations in binary solvent with high pentane/water mole ratio still show aggregation and perovskite formation. The results show that the impact of a relatively small amount of water on perovskite formation is lower than the expected from the well-known instability of the perovskite structure with respect to the presence of moisture. This points out to chemical reactions or solvent-specific interactions as responsible factors for the degradation of on organohalide perovskite films by water.

According to our results the set of force-field parameters that best describe the behavior of precursors in solution does not reproduce accurately the short-range structure of solid perovskite once it is formed. We found that for a better agreement with the crystallographic distances and coordination numbers of solid perovskite a small refinement of the size of the ions in the model is needed.

To summarize, classical Molecular Dynamics can be used as a powerful tool to study perovskite formation with reasonable efforts. This will allow predicting perovskite formation and stability for a variety of novel chemical formulations. A set of force-field parameters that describes well both aggregation and crystalline structure is presented. This will pave the way for designing new structures.

Acknowledgements

We thank Junta de Andalucía for financial support via consolidator programme and grant FQM 1851. We thank Ministerio de Economía y Competitividad of Spain under grant MAT2013-47192-C3-3-R, European Research Council through an ERC Starting Grant

Notes and references

1 A. Kojima, K. Teshima, Y. Shirai and T. Miyasaka, J. Am. Chem. Soc., 2009, 131, 6050–6051.
2 S. Kazim, M. K. Nazeeruddin, M. Grätzel and S. Ahmad, Angew. Chem. Int. Ed. Engl., 2014, 53, 2812–2824.
3 NREL,http://www.nrel.gov/ncpv/images/efficiency_chart.jpg
4 E. J. Juarez-Perez, R. S. Sanchez, L. Badia, G. Garcia-Belmonte, Y. S. Kang, I. Mora-Sero and J. Bisquert, J. Phys. Chem. Lett., 2014, 2390–2394.
5 W. Tress, N. Marinova, T. Moehl, S. M. Zakeeruddin, M. K. Nazeeruddin and M. Grätzel, Energy Environ. Sci., 2015.
6 G. Xing, N. Mathews, S. Sun, S. S. Lim, Y. M. Lam, M. Grätzel, S. Mhaisalkar and T. C. Sum, Science, 2013, 342, 344–347.
7 S. D. Stranks, G. E. Eperon, G. Grancini, C. Menelaou, M. J. P. Alcocer, T. Leijtens, L. M. Herz, A. Petrozza and H. J. Snaith, Science, 2013, 342, 341–344.
8 G. Niu, X. Guo and L. Wang, J. Mater. Chem. A, 2014.
9 N. J. Jeon, J. H. Noh, Y. C. Kim, W. S. Yang, S. Ryu and S. I. Seok, Nat Mater, 2014, 13, 897–903.
10 J. Burschka, N. Pellet, S.-J. Moon, R. Humphry-Baker, P. Gao, M. K. Nazeeruddin and M. Grätzel, Nature, 2013, 499, 316–319.
11 K. Yan, M. Long, T. Zhang, Z. Wei, H. Chen, S. Yang and J. Xu, J. Am. Chem. Soc., 2015, 137, 4460–4468.
12 E. Mosconi, A. Amat, M. K. Nazeeruddin, M. Grätzel and F. De Angelis, J. Phys. Chem. C, 2013, 117, 13902–13913.

13 A. C. T. van Duin, S. Dasgupta, F. Lorant and W. A. Goddard, J. Phys. Chem. A, 2001, 105, 9396–9409.
14 J. D. Deetz and R. Faller, J. Phys. Chem. B, 2014, 118, 10966–10978.
15 S. Hamad, S. Cristol and C. R. A. Catlow, J. Am. Chem. Soc., 2005, 127, 2580–2590.
16 S. Hamad, S. M. Woodley and C. R. A. Catlow, Molecular Simulation, 2009, 35, 1015–1032.
17 N. H. de Leeuw, J. Phys. Chem. B, 2002, 106, 5241–5249.
18 R. Demichelis, P. Raiteri, J. D. Gale, D. Quigley and D. Gebauer, Nat Commun, 2011, 2, 590.
19 J. Anwar and P. K. Boateng, J. Am. Chem. Soc., 1998, 120, 9600–9604.
20 K. Yan, Q. Xue, D. Xia, H. Chen, J. Xie and M. Dong, ACS Nano, 2009, 3, 2235–2240.
21 J. Xie, Q. Xue, K. Yan, H. Chen, D. Xia and M. Dong, J. Phys. Chem. C, 2009, 113, 14747–14752.
22 J. M. Frost, K. T. Butler and A. Walsh, APL Materials, 2014, 2, 081506.
23 H. J. C. Berendsen, J. R. Grigera and T. P. Straatsma, J. Phys. Chem., 1987, 91, 6269–6271.
24 C. Oostenbrink, A. Villa, A. E. Mark and W. F. van Gunsteren, J Comput Chem, 2004, 25, 1656–1676.
25 M. G. Martin and J. I. Siepmann, J. Phys. Chem. B, 1998, 102, 2569–2577.
26 N. US Department of Commerce, 2015, www.nist.gov/srd
27 Y. Won, J. Phys. Chem. A, 2012, 116, 11763–11767.
28 G. Markovich, L. Perera, M. L. Berkowitz and O. Cheshnovsky, The Journal of Chemical Physics, 1996, 105, 2675–2685.
29 N. C. for B. Information, U. S. N. L. of Medicine and 8600 Rockville Pike, Bethesda, MD20894, and USA, .
30 J. Wang, R. M. Wolf, J. W. Caldwell, P. A. Kollman and D. A. Case, J. Comput. Chem., 2004, 25, 1157–1174
31
32 E. C. Meng and P. A. Kollman, J. Phys. Chem., 1996, 100, 11460–11470.
33 J. M. Vicent-Luna, J. Idígoras, S. Hamad, S. Calero and J. A. Anta, J. Phys. Chem. C, 2014, 118, 28448–28455.
34 S. Pronk, S. Páll, R. Schulz, P. Larsson, P. Bjelkmar, R. Apostolov, M. R. Shirts, J. C. Smith, P. M. Kasson, D. van der Spoel, B. Hess and E. Lindahl, Bioinformatics, 2013, 29, 845.
35 J.-P. Hansen and I. R. McDonald, Theory of Simple Liquids, Second Edition, Academic Press, 2 edition., 1990.
36 K. G. Stamplecoskie, J. S. Manser and P. V. Kamat, Energy Environ. Sci., 2014, 8, 208–215.
37 Y. Dang, Y. Liu, Y. Sun, D. Yuan, X. Liu, W. Lu, G. Liu, H. Xia and X. Tao, CrystEngComm, 2014, 17, 665–670.
38 B. C. O'Regan, P. R. F. Barnes, X. Li, C. Law, E. Palomares and J. M. Marin-Beloqui, J. Am. Chem. Soc., 2015, 137, 5087–5099.
39 R. S. Sanchez, V. Gonzalez-Pedro, J.-W. Lee, N.-G. Park, Y. S. Kang, I. Mora-Sero and J. Bisquert, J. Phys. Chem. Lett., 2014, 2357–2363.
40 E. L. Unger, E. T. Hoke, C. D. Bailie, W. H. Nguyen, A. R. Bowring, T. Heumüller, M. G. Christoforo and M. D. McGehee, Energy Environ. Sci., 2014, 7, 3690–3698.
41 J. M. Frost, K. T. Butler, F. Brivio, C. H. Hendon, M. van Schilfgaarde and A. Walsh, Nano Lett., 2014, 14, 2584–2590.
42 D. ben-Avraham and S. Havlin, Diffusion and Reactions in Fractals and Disordered Systems, Cambridge University Press, Cambridge, 2000.
43 J. A. Christians, P. A. Miranda Herrera and P. V. Kamat, J. Am. Chem. Soc., 2015, 137, 1530–1538.
44 J. Yang, B. D. Siempelkamp, D. Liu and T. L. Kelly, ACS Nano, 2015, 9, 1955–1963.
45 J. Anta, E. Lomba and M. Lombardero, Physical Review E, 1997, 55, 2707.